nature portfolio

Peer Review File

ALKBH5 acts as a facilitator for hair follicle telogen-to-anagen transition

Corresponding Author: Professor Ying Lin

Parts of this Peer Review File have been redacted as indicated to remove third-party material.

This file contains all reviewer reports in order by version, followed by all author rebuttals in order by version.

Version 0:

Reviewer comments:

Reviewer #1

(Remarks to the Author)
Lin and colleagues study the role of ALKBH5 and the N6-methyladenosine (M6A) modification in hair follicle stem cell (HFSC) activation during telogen-to-anagen transition. Deletion of murine Alkbh5 in epithelial tissues using K5-CreERT2 or Lgr5-CreERT2 resulted in a slightly accelerated telogen-to-anagen transition and increased HFSC proliferation. The authors propose Mcam as a target of ALKBH5, providing evidence that the deletion of Alkbh5 results in increased M6A levels on the Mcam transcript, leading to a higher expression of MCAM. Finally, they show that the silencing of Mcam in vitro leads to reduced cell proliferation. Overall, this is an interesting study, clearly demonstrating the involvement of ALKBH5 in HFs growth. The connection between ALKBH5 to MCAM and hair cycling is rather loose and it is not well-supported by experimental data.

Comments:
1. The authors focus here on intrinsic roles of ALKBH5 in HFSCs. However, the deletion of Alkbh5 using K5-Cre resulted in a stronger phenotype compared to the Lgr5-Cre mice. This indicates that ALKBH5 activity may also have extrinsic effects on HFSCs. Another issue is the fact that the deletion of Alkbh5 in both of these genetic models was done systemically, thus resulting in the deletion of Alkbh5 in wide-ranging cell types and tissues not restricted only to skin epithelium.

2. RNA-seq analysis is too preliminary; samples size (n=1) is too small to allow any robust insights on the transcriptional changes. Informative description of RNA-seq analysis is missing in the manuscript methods text. Does cells used for this analysis obtained from K5-Cre and if so, how cell-extrinsic effects can be excluded in such a case? How were the differentially expressed genes determined? In addition, it is impossible to evaluate this data as the list of differentially expressed genes is not included in manuscript files.
3. Analysis of M6A analysis is too preliminary; only a single replicate for each condition was used, with a 20-fold difference in the number of cells used in each group ("5×10^3–1×10^5"). The numbers of cells used in control and cKO should have been similar, and experimental pipeline should also include internal normalization controls to accommodate for downstream processes. Finally, the high background shown for input sample strongly indicates that library preparation process was somewhat problematic and data may contain false positive signal.
4. Mechanistic connection between MCAM and the hair cycle phenotype is unclear; Does MCAM expression dynamically changes during hair cycle stages in control mice? Does its overexpression in cultures cells affects Wnt signaling component as authors suggest, and if so which genes?
5. Following the previous comment, the authors established that Alkbh5 deletion leads to increased MCAM, but their in vitro analysis is out of context and focused on the cellular effects upon MCAM silencing. Authors should analyze the effect of MCAM overexpression.
6. Images in several histology panels use show disrupted tissue and/or image is out of focus (for example see Figs. 2D, S1B, S1D, S1H).
7. The deletion of Alkbh5 (Fig. 1C) should be evaluated more broadly over a larger skin area and not restricted to a single HF in order to provide a sense of how robust in the genetic deletion.

Reviewer #2

(Remarks to the Author)
It is known that hair cycle transition is important for hair growth, particularly the switch from telogen to anagen. This article explored the regulatory mechanism of Alkbh5 in HFSCs and mice. The result indicates that ALKBH5 regulates Mcam expression mediated by m6A methylation to activate HFSC to maintain the hair cycle, which is helpful for therapeutic strategies on hair regeneration and tissue repair. Although the authors provide many detailed results in vivo and in vitro, there are still some specific comments as belows.
1. The writing style of MCAM and Mcam should be consistent.
2. Please explain Bu, HG and DP in figure 1C legend. Figure1I is the Immunofluorescence staining for EdU result in skin tissues from A5 cKO and A5 Ctrl mice at P56 and P68, but in this figure legend is P69. As the design of this study (Figure 1B), it should be P69. Please keep it consistent.
3. From figure1B and figure 2A, the mice are different. However, the authors used the same name in figure 2. In Addition, please add corresponding group names under the bars in figure 2B. The label of knockout mice in figure 2C are not consistent with figure legend.
4. In figure 3F, the right is the quantification of sphere diameters at day 0, 1, 3, 5,10, while in this figure legend, the days are 1, 3, 7, and 10. They are not matched.
5. In figure 3H, the left is the quantification result, the right is the immunofluorescence result. Not as the authors' description in figure 3H legend.
6. The figure 5D is not clear.
7. The name of real time quantitative PCR was not consistent, such as in the tile was qRT-PCR, while in the text, it is qPCR.
8. There was no primer sequence information in this manuscript.
9. It is better to provide a regulatory mechanism diagram in the text.
10. There are a lot of mistakes in the manuscript, especially in result part. The figure legends were not well matched with the figures as the above described, which is not easy to understand.

Reviewer #3

(Remarks to the Author)
This manuscript by Chen et al. presents a compelling investigation into the role of the RNA demethylase ALKBH5 in regulating hair follicle stem cell (HFSC) activation during the telogen-to-anagen transition. The study combines in vivo genetic models, in vitro functional assays, and multi-omics approaches to demonstrate that ALKBH5-mediated m6A demethylation of Mcam mRNA serves as an intrinsic checkpoint for HFSC proliferation. The work is well-structured, methodologically rigorous, and addresses a significant gap in understanding how epitranscriptomic mechanisms fine-tune stem cell behavior in cyclic tissue regeneration. The findings have potential implications for treating hair loss disorders. While the mechanistic link between MCAM and Wnt signaling requires further exploration, the study is rigorously executed and merits publication pending minor revisions. The findings will interest researchers in regenerative biology, epitranscriptomics, and dermatology.

1. Since m6A modification is dynamically regulated in vivo, does Mettl3 cooperate with Alkbh5 to regulate the hair cycle and the proliferation phenotype of hair follicle stem cells in mice?
2. Is Mcam a target gene jointly regulated by Mettl3 and Alkbh5?
3. Does Alkbh5 knockout promote periodic activation and proliferation of hair follicle stem cells in mice, and could this ultimately result in an exhausted hair follicle stem cell pool?
4. Please perform experiments by testing if MCAM knockdown suppresses Wnt target genes (e.g., Axin2, Cyclin D1) or alters β-catenin localization in HFSCs.
5. Please assess MCAM's role in HFSC migration/niche engagement via live imaging or transwell assays.
6. Both Alkbh5 and Fto are demethylases. While the expression of Alkbh5 is shown to change during the transition of the hair follicle cycle in mice, does Fto expression also change during this process?
7. To validate the consistency of cellular phenotypes in vivo and in vitro, does Alkbh5 knockout affect the apoptosis of hair follicle stem cells in 3D cultures?
8. Please specify the number of alopecia areata patient samples used in scRNA-seq analysis to bolster translational claims.

Version 1:

Reviewer comments:

Reviewer #1

(Remarks to the Author)
This reviewer appreciates the efforts made by the authors to address comments raised. While authors indeed addressed a substantial part of my comments and much improved the revised manuscript, a major concern remains the data interpretation related to comment #1.
The manuscript must not state "cell-intrinsic" role for ALKBH5 in HFSCs, as the experimental data clearly shows that a broader epidermal deletion using the K5-CreERT2 model results in a much robust phenotype comparing to the HFSC-specific deletion using the Lgr5-CreERT2 model. It is possible that a better experimental design for the deletion of ALKBH5 in HFSCs could result in a similar phenotype to the K5-CreERT2 model, but this was not demonstrated and remains

speculative. Since authors used the K5-CreERT2 model throughout majority of their paper, they should adhere to the experimental data in a conservative manner, and this should be reflected in the revised text and discussion more clearly.

Reviewer #3

(Remarks to the Author)
The authors have fully addressed my questions.

Author's Response to Review #1：

1. The authors focus here on intrinsic roles of ALKBH5 in HFSCs. However, the deletion of Alkbh5 using K5-Cre resulted in a stronger phenotype compared to the Lgr5-Cre mice. This indicates that ALKBH5 activity may also have extrinsic effects on HFSCs. Another issue is the fact that the deletion of Alkbh5 in both of these genetic models was done systemically, thus resulting in the deletion of Alkbh5 in wide-ranging cell types and tissues not restricted only to skin epithelium.

   We thank the reviewer for this important comment. We agree that the stronger phenotype observed in the Krt5-CreERT2 model compared with the Lgr5-CreERT2 model raises the possibility that ALKBH5 may also act through non-HFSC epithelial compartments or local epithelial niche interactions. We did not intend to exclude this possibility, rather, our study focuses primarily on the cell-intrinsic regulatory role of ALKBH5. In our study, the Krt5-CreERT2 model was used to delete Alkbh5 broadly in epidermal and follicular epithelial cells, whereas the Lgr5-CreERT2 model allowed us to examine the effect of Alkbh5 deletion in a more restricted HFSC population (Fig. S2A,B). Similar differences in phenotypic severity resulting from deletion of the same gene in different cellular compartments have also been reported in other studies. For example, in studies investigating the function of BMP signaling in epithelial cells, K5-Cre-mediated deletion produced a stronger and more widespread phenotype than Lgr5-Cre-mediated deletion[1,2] (Thomas Andl *et al* (2002). *Development*. 2(5):643-53; Elena Kandyba *et al* (2013). *PNAS*. 110(4):1351-6). Alternatively, Alkbh5 may regulate the expression of secreted factors in epithelial cells outside the HFSC compartment, thereby indirectly influencing HFSC activity. previous studies have shown that m^{6}A modification can modulate the expression of secreted factors in skin epithelial cells, consequently shaping the local inflammatory microenvironment[3] (Cui L *et al* (2024). *Sci Adv*. 10(40):eadp5332). This point has been addressed and included in the Discussion section of our revised text.

   While we acknowledge that these genetic models may involve systemic effects, the consistency across our independent experimental approaches—particularly the accelerated telogen-to-anagen transition observed in both *Krt5* and *Lgr5* Cre models (Fig 1 and Fig 2), the localized effects of ALKBH5 pharmacological inhibition (Fig S3), and the cell-autonomous proliferation observed *in vitro* (Fig 3), we believe the conclusion that ALKBH5 functions, as an intrinsic regulator of HFSCs.

   We have now integrated the relevant discussion into the fifth paragraph of the

Discussion section : **The more pronounced phenotype observed in Krt5CreERT2 mice compared to Lgr5CreERT2 mice likely stems from the additional deletion of Alkbh5 in the epidermis, which could potentially impact the HFSC microenvironment through extrinsic signals. However, the finding that in vitro cultured HFSCs still exhibit altered activation and proliferation upon Alkbh5 deficiency provides compelling evidence that Alkbh5 primarily acts as an intrinsic regulator of HFSCs, independent of systemic or niche-derived influences. Nevertheless, this still cannot completely rule out the possibility that Alkbh5 exerts cell-extrinsic regulatory effects, because in vivo phenotypes result from the coordinated actions of cell-intrinsic mechanisms and the microenvironment. Our current experimental approaches cannot comprehensively capture all potential regulatory mechanisms.**

2. RNA-seq analysis is too preliminary; samples size (n=1) is too small to allow any robust insights on the transcriptional changes. Informative description of RNA-seq analysis is missing in the manuscript methods text. Does cells used for this analysis obtained from K5-Cre and if so, how cell-extrinsic effects can be excluded in such a case? How were the differentially expressed genes determined? In addition, it is impossible to evaluate this data as the list of differentially expressed genes is not included in manuscript files.

   We apologize for the preliminary nature of the initial RNA-seq data. As suggested, we have now performed additional RNA-seq experiments to increase the sample size to n=3 per group. The updated analysis, which now allows for robust statistical insights, has been incorporated into the revised manuscript, and performed below in Fig 4A, Fig S5A, B. The cells used for RNA-seq were FACS-sorted HFSCs isolated from late-telogen Krt5- CreERT2 mice and littermate control mice. Based on the consistent phenotypes observed in different Cre mouse models, together with the results from in vitro culture of sorted HFSCs, we believe that the RNA-seq data obtained from the Krt5-CreERT2 model can reflect that cell-intrinsic effects of *Alkbh5* deletion. We have added a detailed description of the RNA-seq library preparation, sequencing platform, and bioinformatics pipeline in the 'Materials and Methods' section ： **For RNA-seq, raw paired-end sequencing data were first processed using fastp to remove low-quality bases and sequencing adapters. The cleaned high-quality reads were then aligned to the mouse reference genome (GRCm39) using HISAT2. Alignment outputs were directly piped to SAMtools for BAM format conversion, coordinate sorting, and index generation. Gene-level quantification was subsequently performed using the**

featureCounts function from the Subread package based on the GENCODE (vM32) genome annotation file, by counting reads mapped to exonic regions. The resulting expression matrix was used for downstream differential expression analysis. After preprocessing and gene annotation, the raw gene count matrix was subjected to differential expression analysis. Samples were grouped according to genotype into WT and cKO groups, and batch information was included to correct for potential batch effects. Differential expression analysis was performed using the PyDESeq2 package in Python with the statistical design formula: count ~ batch + condition, where condition was used to compare expression differences between cKO and WT samples, and batch was used to account for batch effects. PyDESeq2 performed size-factor normalization, dispersion estimation, and negative binomial generalized linear model fitting on the raw count data, followed by Wald tests to evaluate expression changes in cKO relative to WT samples. Differentially expressed genes (DEGs) were identified using the thresholds of p value < 0.05 and |log2FoldChange| > 1. Pathway enrichment analysis was conducted using gseapy based on the GO, KEGG, Reactome, and WikiPathways databases to separately analyze enriched pathways among upregulated and downregulated genes.

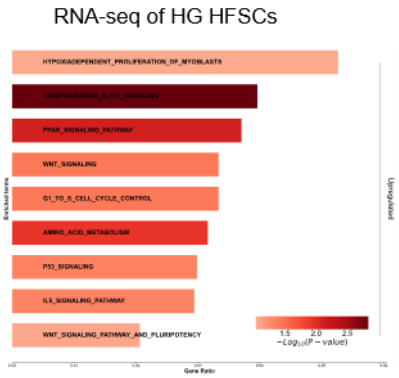

Figure 4 ALKBH5 regulates *Mcam* transcript stability through its demethylase activity. (A) KEGG pathway enrichment analysis of upregulated and downregulated genes in hair germ (HG) region HFSCs from A5;K5-Ctrl and A5;K5-cKO mice (n=3 per group).

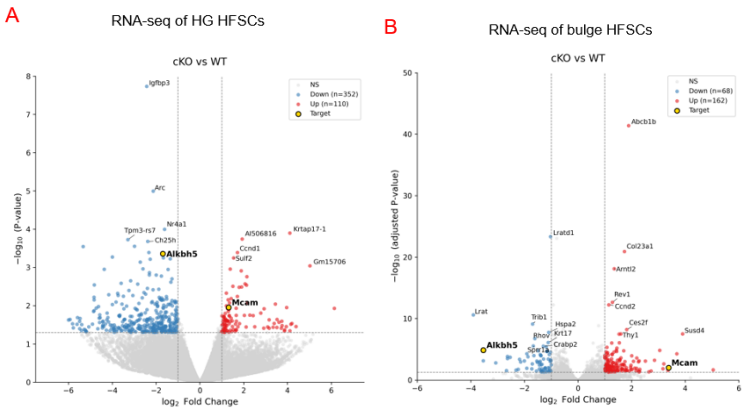

Figure S5 ALKBH5 regulates *Mcam* transcript stability and expression. (A) Volcano plot showing differentially expressed genes between wild-type (WT, n = 3) and *Alkbh5*-deficient (n = 3) hair germ (HG) HFSCs. Red dots indicate upregulated genes, and blue dots indicate downregulated genes. (B) Volcano plot showing differentially expressed genes between WT (n = 4) and *Alkbh5*-deficient (n = 4) bulge-region HFSCs. Red dots represent upregulated genes, and blue dots represent downregulated genes.

Differentially expressed genes (DEGs) were identified using DESeq2. The threshold for significance was set at an p-value < 0.05 and a fold change >2. We have detailed these criteria in the revised Methods section. The complete list of differentially expressed genes, including fold changes and p-values, is now **provided as "DEGs of RNA-seq" of Supplementary Table S1.**

3. Analysis of m^{6}A analysis is too preliminary; only a single replicate for each condition was used, with a 20-fold difference in the number of cells used in each group ("5x10^3-1x10^5"). The numbers of cells used in control and cKO should have been similar, and experimental pipeline should also include internal normalization controls to accommodate for downstream processes. Finally, the high background shown for input sample strongly indicates that library preparation process was somewhat problematic and data may contain false positive signal.

   We apologize for the confusion caused by our description of the cell numbers. The referenced low-input MeRIP-seq protocol suggests a starting material as low as 5x10^3 cells; accordingly, we conducted pilot experiments across a range of 5x10^3 to 1x10^5 cells to verify the technical feasibility. However, we determined that 1x10^4 cells yielded the most optimal and reproducible results. Therefore, all formal experiments were consistently performed using a fixed starting population of 1x10^4 cells per sample. The range mentioned in our previous Methods section was intended to describe the applicable scope of this low-input library preparation method : **For each sample with m6A-CT-seq, 1×104 HFSCs were washed twice with 100 μL of Wash Buffer (20 mM HEPES, PH=7.5).**

Regarding the internal normalization, we wish to clarify that while exogenous spike-in RNA were not introduced, we implemented a rigorous normalization strategy to ensure the comparability of m^{6}A enrichment levels between groups. While spike-in controls are considered the gold standard for quantitative MeRIP-seq, their introduction into ultra-low-input samples may introduce additional handling loss or dilution errors. Consequently, we adopted a more cautious strategy centered on standardization of starting material combined with internal control validation to ensure the maximal integrity and reproducibility of our endogenous m^{6}A signals. First, we strictly standardized the starting material by using an identical number of HFSCs (1x10^4) and equal amounts of total RNA for both the Control and cKO groups during the MeRIP process. Second, during bioinformatic analysis, we utilized “BPM” to normalize for library size and sequencing depth across samples. Subsequent IP/Input peak-calling analysis was performed using exomePeak2. Crucially, our analysis revealed a robust enrichment of the classical m^{6}A consensus motif (RRACH), indicating high specificity in our m^{6}A-seq results (Fig S5C). Most importantly, to validate the m^{6}A-seq findings, we performed independent MeRIP-qPCR for our key candidate genes (e.g., *Mcam*), which consistently recapitulated the changes observed in our sequencing data. This cross-validation effectively demonstrates that our experimental pipeline, even without spike-in RNA, provides reliable and reproducible insights into the m^{6}A methylome.

The low-input m^{6}A-seq approach used in our study was adapted from the method published in *Molecular Cell* in 2023, namely single-nucleus m^{6}A-CT-seq, which is based on the CUT&Tag principle[4]（Hamashima K *et al* (2023). *Mol Cell*. S1097-2765(23)00649-4). This method is suitable for samples with limited cell numbers and can serve as a discovery approach to identify candidate m^{6}A-regulated transcripts. Based on this principle, during library construction, Tn5 transposase can fragment nearby double-stranded molecules, including DNA/RNA hybrid duplexes or double-stranded DNA, which may generate background signals, particularly in low-input library preparation. In addition, a systematic comparison of different single-cell m^{6}A-seq methods has indicated that the signal-to-background ratio of m^{6}A-CT-seq depends, at least in part, on the specificity of the m^{6}A antibody[5] (Li, Y *et al* (2025). *Commun Biol*. 8, 1841). These factors may explain the relatively high background observed in our m^{6}A-CT-seq data. Nevertheless, we further validated the candidate target gene identified from the sequencing analysis, *Mcam*, using independent approaches, including MeRIP-qPCR, mRNA half-life assays, and ALKBH5 rescue experiments. To further ensure experimental rigor, we

performed an additional validation using an alternative low-input m^{6}A-seq method, picoMeRIP-seq, which showed a lower background signal[6] (Li Y et al (2024). *Nat Biotechnol*. 42(4):591-596). Importantly, *Mcam* was again identified among the differential candidate genes in this independent dataset, as shown in the fig 4C.

We have added a detailed description of the MeRIP-seq library preparation, bioinformatics pipeline : **The m^{6}A-seq libraries were constructed following the picoMeRIP-seq protocol with minor modifications. Briefly, 1 μg of anti-m^{6}A antibody (CST, 56593) was conjugated with 10 μg of Dynabeads Protein G (Invitrogen, 3095287) by incubation at 4°C for 2 hours, followed by resuspension in 20 μl of IP buffer. For RNA fragmentation, 50 ng of total RNA was subjected to low-temperature water-bath sonication (QSONICA, Q800R3; 30 s on/30 s off, 3 cycles at 27% power). The fragmented RNA was then incubated with the antibody-bead complexes at 4°C for 2 hours. The beads were sequentially washed three times with ice-cold IP buffer, three times with low-salt buffer, and three times with high-salt buffer. The m6A-enriched RNA was eluted twice using 50 μl of RLT lysis buffer (Qiagen, 169038865) and subsequently purified using RNA Clean Beads (Vazyme, #N412-02-AA). The downstream library construction was performed using the AG Low-input RNA Transcriptome Library Prep Kit (AG, AG12526) according to the manufacturer's instructions. Finally, high-throughput sequencing was conducted on the NovaSeq X Plus platform (Illumina) in a paired-end 150 bp (PE150) mode.**

For MeRIP-seq data analysis, raw paired-end sequencing reads were first processed using fastp with default parameters for quality control, including removal of adapter sequences and low-quality bases. The cleaned high-quality reads were then aligned to the mouse reference genome (GRCm39) using HISAT2 under default settings. The resulting SAM files were converted to BAM format using SAMtools, followed by coordinate sorting and index generation. Alignment statistics were generated using the samtools flagstat command. For downstream genome visualization, the sorted BAM files were converted into BigWig format using the bamCoverage function from the deepTools package, with a bin size of 10 bp and normalization performed using the "BPM" (Bins Per Million mapped reads) method. Subsequent IP/Input peak-calling analysis was performed using exomePeak2.

C

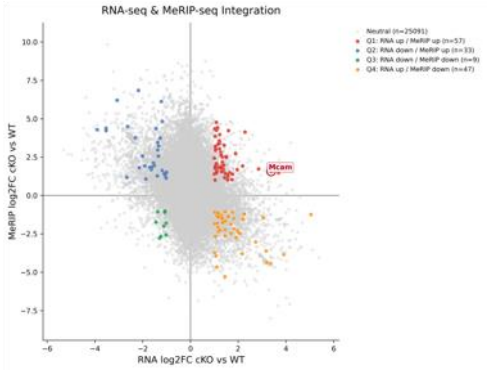

Figure 4 ALKBH5 regulates Mcam transcript stability through its demethylase activity. (C) Integrated analysis of A5;K5 mice RNA-seq and m^{6}A-seq data from bulge-region HFSCs showing the intersection of differentially expressed genes and genes with altered m^{6}A modification. The “RNA” indicates the expression level of transcripts, the “peak” indicates the level of m^{6}A modification. (n=3 per group).

4. Mechanistic connection between MCAM and the hair cycle phenotype is unclear; Does MCAM expression dynamically changes during hair cycle stages in control mice? Does its overexpression in cultures cells affects Wnt signaling component as authors suggest, and if so which genes?

   We thank the reviewer for this important comment. We agree that the mechanistic connection between MCAM and the hair cycle phenotype was not sufficiently established in the original manuscript. We have previously analyzed the transcript levels of *Mcam* in HFSCs during early and late telogen using RT-qPCR, as presented in Fig.5A. Following your insightful suggestion, we have now supplemented our findings with immunofluorescence staining to examine MCAM protein expression during these stages, as shown in Fig.5B. The results demonstrate that the protein levels of MCAM are highly consistent with the observed transcriptional changes, further strengthening the robustness of our data. These new results have been incorporated into the revised manuscript.

   We further investigated whether *Mcam* modulates Wnt signaling, a regulator of HFSC activation. By knocking down *Mcam* in primary HFSCs isolated from Control and *Alkbh5* cKO mice to perform rescue experiments, and upon treatment with WNT1, we observed that the upregulation of Wnt signaling target genes, including Cyclin D1(*Ccnd1*), Cyclin D2(*Ccnd2*), *Ppard*. The expression of Wnt downstream target genes was higher in *Alkbh5* cKO cells than in control cells, whereas *Mcam* knockdown reduced the expression of these target genes, as shown in Fig.5G. These findings provide a potential mechanistic link between ALKBH5-mediated *Mcam* regulation and the downstream activation of the Wnt pathway.

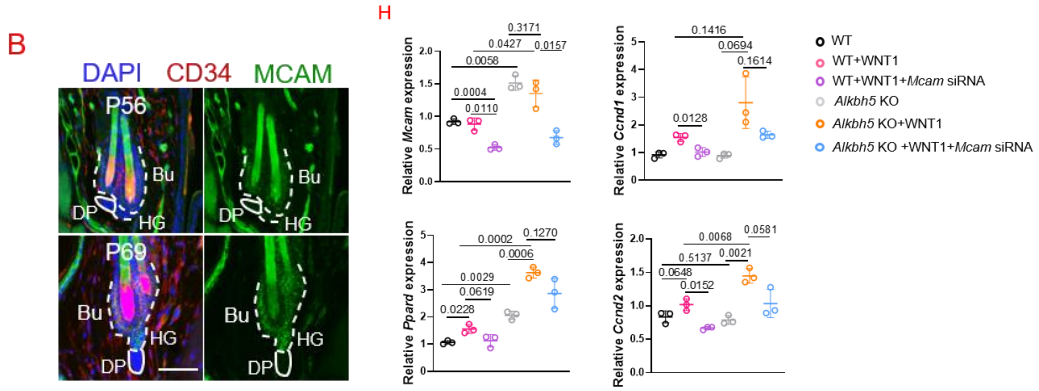

Figure 5 MCAM promotes hair follicle stem cell proliferation. (B) Immunofluorescence staining of MCAM protein in mouse HFSCs at the early (P56, n = 5) and late (P69, n = 5) telogen phases. (H) RT-qPCR analysis of the expression levels of the Wnt target genes *Ccnd1*, *Ccnd2*, and *Ppard* in A5;K5-Ctrl, A5;K5-cKO, *Mcam*-knockdown A5;K5-Ctrl, and *Mcam*-knockdown A5;K5-cKO HFSCs under both untreated and WNT1-treated conditions.

5. Following the previous comment, the authors established that Alkbh5 deletion leads to increased MCAM, but their in vitro analysis is out of context and focused on the cellular effects upon MCAM silencing. Authors should analyze the effect of MCAM overexpression.

   We sincerely appreciate the reviewer's constructive feedback. To complement our initial knockdown experiments that demonstrated the necessity of MCAM, we have performed overexpression assays in primary HFSCs to further establish its sufficiency in driving the observed phenotypes. Considering the inherently low transfection efficiency of primary cells, which is further exacerbated in a 3D Matrigel culture environment, we performed the MCAM overexpression experiments using primary HFSCs under 2D culture conditions. To ensure accurate analysis, we employed fluorescence-activated cell sorting (FACS) to specifically isolate the transfected cells (mCherry-positive) for verifying the overexpression efficiency via RT-qPCR. Under these validated conditions, we conducted EdU incorporation assays, which revealed that MCAM overexpression significantly promotes HFSC proliferation. These findings are consistent with our MCAM knockdown results and are presented in Fig.5G.

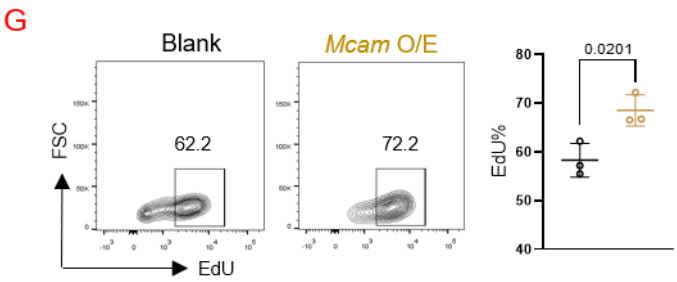

Figure 5 MCAM promotes hair follicle stem cell proliferation. (G) Flow cytometric analysis of the percentage of EdU^{+} cells in primary HFSCs overexpressing Mcam or carrying the empty vector control.

6. Images in several histology panels use show disrupted tissue and/or image is out of focus(for example see Figs.2D,S1B,S1D,S1H).

   We apologize for the suboptimal quality of the histology images in the original manuscript. We appreciate the reviewer's careful inspection of our data. In accordance with your comments, we have meticulously reviewed all histology panels. We have now replaced the low-quality images (including Figs. 2D, S1B, S1D, and S1H) with new, high-quality micrographs that feature intact tissue morphology and sharp focus.

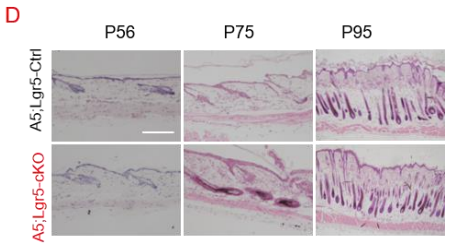

Figure 2 Alkbh5 ablation in hair follicle stem cells promotes their activation. (D) H&E staining of dorsal skin from A5; Lgr5-cKO and A5; Lgr5 Ctrl mice at P56, P75, and P105. Scale bar, 200 μm.

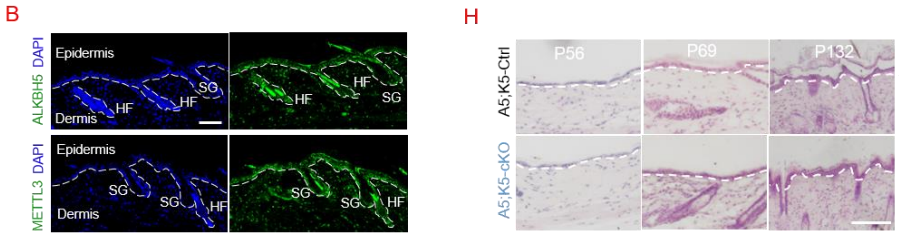

Figure S1 Hair cycle progression in *Alkbh5* knock out mice over time. (B) Immunofluoresence staining of DAPI (Blue), ALKBH5 (Green) and METTL3 (Green) in mouse skin (n = 3) at P56. The white dashed line delineates the epidermis (Epidermis) from the hair follicle (HF). Scale bar, 50 μm. (H) Hematoxylin and eosin (H&E) staining of skin sections from A5;K5-cKO and A5;K5-Ctrl mice (n = 3) at P56, P68, and P132.

7. The deletion of Alkbh5(Fig.1C) should be evaluated more broadly over a larger skin area and not restricted to a single HF in order to provide a sense of how robust in the genetic deletion.

   We thank the reviewer for this constructive suggestion regarding the evaluation of Alkbh5 deletion efficiency. To demonstrate the robustness of our genetic model, we have now provided broader histological views and are shown in Fig. 1B.

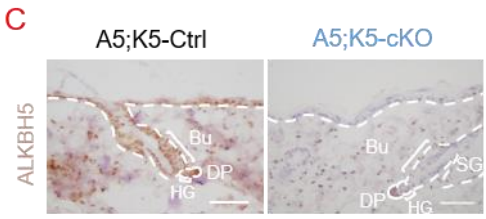

Figure 1 Alkbh5 knockout promotes telogen-to-anagen transition in hair follicles. (C) Immunohistochemical staining for ALKBH5 in P56 skin tissues (n = 3) to assess knockout efficiency following tamoxifen induction. Scale bar, 50 μm. Bu indicates the bulge region of HFSCs; HG indicates the hair germ of HFSCs; DP indicates the dermal papillae.

Author's Response to Reviewer #2

1. The writing style of MCAM and Mcam should be consistent.

   We thank the reviewer for pointing this out. We have carefully checked the manuscript and revised the nomenclature throughout the text to ensure consistency. Specifically, *Mcam* is now used when referring to the mouse gene or mRNA, whereas MCAM is used when referring to the protein. The figure labels, legends, and supplementary tables have been revised accordingly.

2. Please explain Bu, HG and DP in figure 1C legend. Figure 1I is the Immunofluoresence staining for EdU result in skin tissues from A5 cKO and A5 Ctrl mice at P56 and P68, but in this figure legend is P69. As the design of this study (Figure 1B), it should be P69. Please keep it consistent.

   We thank the reviewer for pointing this out. The descriptions mentioned above have been modified accordingly in the revised manuscript. The figure 1C legend of revised manuscript: **(C) Immunohistochemical staining for ALKBH5 in P56 skin tissues (n = 3) to assess knockout efficiency following tamoxifen induction. Scale bar, 50 μm. Bu indicates the bulge region of HFSCs; HG indicates the hair germ of HFSCs; DP indicates the dermal papillae.**

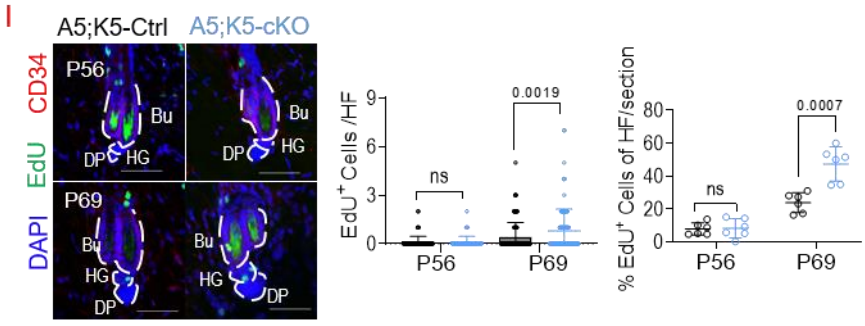

Figure 1 Alkbh5 knockout promotes telogen-to-anagen transition in hair follicles. (I) (Left) Immunofluorescence staining for EdU (green), CD34 (red), and DAPI (blue) in skin tissues from A5;K5-cKO and

A5;K5-Ctrl mice (n = 6) at P56 and P69. Scale bar, 50 μm. (Right) Quantification of absolute numbers and percentages of EdU^+ HFSCs.

3. From figure 1B and figure 2, the mice are different. However, the authors used the same name in figure 2. In addition, please add corresponding group names under the bars in figure 2B. The label of knockout mice in figure 2C are not consistent with figure legend.

   We thank the reviewer for pointing this out. In the original experimental workflow diagrams in Fig. 1B and Fig. 2A, we indicated that blue represents A5;K5 mice and red represents A5;Lgr5 mice. However, we agree that revising the figure according to your suggestion will make it clearer and more reader-friendly. Samples from *Krt5*^{CreERT2} mice are labeled in blue and abbreviated as A5;K5-Ctrl and A5;K5-cKO (Fig 1B), whereas samples from *Lgr5*^{CreERT2} mice are labeled in red and abbreviated as A5;Lgr5-Ctrl and A5;Lgr5-cKO (Fig 2A).

[figure redacted]

Figure 1 Alkbh5 knockout promotes telogen-to-anagen transition in hair follicles. (B) *Alkbh5*$^{fl/fl}$; *Krt5*$^{CreERT2+/-}$ conditional knockout (A5;K5-cKO) and *Krt5*$^{CreERT2+/-}$ control (A5;K5-Ctrl) mice received intraperitoneal tamoxifen injections for four consecutive days starting at P42, and skin samples were collected at P56 and P69. The period from P42 to P69 corresponds to the second telogen phase of the hair cycle.

[figured redacted]

Figure 2 *Alkbh5* ablation in hair follicle stem cells promotes their activation. (A) Schematic diagram showing the timeline of tamoxifen intraperitoneal injection. Skin tissues were collected at P56 and P69. The period from P42 to P69 corresponds to the second telogen phase of the mouse hair cycle. Black circles indicate *Lgr5*$^{EGFP\text{-}Ires\text{-}CreERT2+/-}$ control mice (A5; Lgr5-Ctrl), and red circles indicate *Alkbh5*$^{fl/fl}$; Lgr5$^{EGFP\text{-}Ires\text{-}CreERT2+/-}$ conditional knockout mice (A5; Lgr5-cKO).

4. In figure 3F, the right is the quantification of sphere diameters at day 0, 1, 3, 5, 10, while in this figure legend, the days are 1, 3, 7, and 10. They are not matched.

We sincerely thank the reviewer for the careful reading of our manuscript and for pointing out the issues that required correction. We have corrected this writing error in the figure.

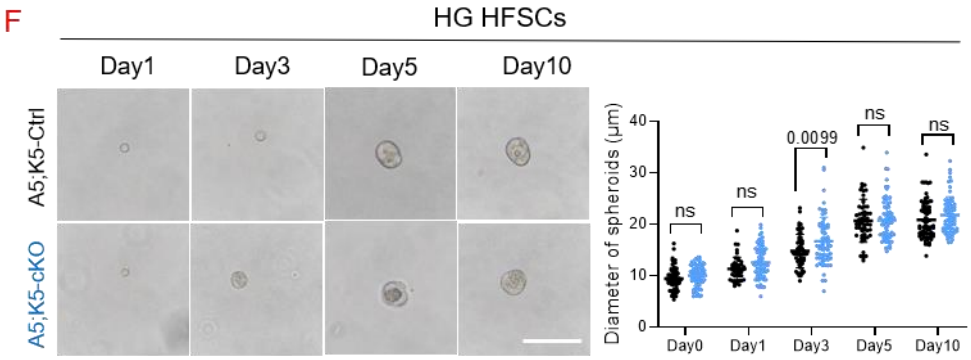

Figure 3 *Alkbh5* knockout accelerates early-stage proliferation of hair follicle stem cells in vitro. (F) (Left) Representative bright-field images of 3D-cultured HFSCs from A5;K5-cKO and A5;K5-Ctrl mice (n = 3) at day 1, 3, 5 and 10. Scale bar, 50 μm. (Right) Quantification of sphere diameters at day 0, 1, 3, 5 and 10 of HG-region HFSC 3D cultures.

5. In figure 3H, the left is the quantification result, the right is the immunofluorescence result. Not as the authors' description in figure 3H legend.

We sincerely thank the reviewer for the careful reading of our manuscript and for pointing out the writing error that required correction. And it has now been corrected.

6. The figure 5D is not clear.

We thank the reviewer for pointing this out. It has now been replaced with a image of high resolution.

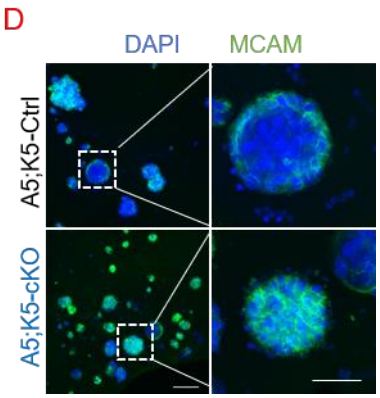

Figure 5 MCAM promotes hair follicle stem cell proliferation. (D) (Left) Immunofluorescence staining of 3D-cultured HFSC spheres for MCAM (green), CD34 (red), and DAPI (blue), showing elevated MCAM protein levels

following Alkbh5 deletion. Scale bar, 100 μm. (Right) The right panel show magnified views of the white boxes in the images on the left. Scale bar, 50 μm.

7. The name of real time quantitative PCR was not consistent, such as in the tile was RT-qPCR, while in the text, it is qPCR.
   We thank the reviewer for pointing thie out. All instances of “qPCR” in the main text have now been revised to “RT-qPCR.”

8. There was no primer sequence information in this manuscript.
   We thank the reviewer for pointing this out. In fact, we have included the primer sequence in Supplementary Table1.

9. It is better to provide a regulatory mechanism diagram in text.
   We thank the reviewer for pointing this out. According to your suggestion, we have added a regulatory mechanism diagram to the manuscript, which enables readers to better understand the research content.

[figure redacted]

10. There are a lot of mistakes in the manuscript, especially in the result part. The figure legends were not well matched with the figures as the above described, which is not easy to understand.

    We sincerely thank the reviewer for the careful reading of our manuscript and for pointing out these issues. We apologize for the mistakes and inconsistencies in the Results section and figure legends. According to the reviewer's suggestions, we have carefully rechecked the entire manuscript and thoroughly revised the relevant text and figure legends to ensure that they accurately correspond to the figures and are easier to understand. We have also corrected the language and formatting errors throughout the manuscript.

Author's Response to Reviewer #3

1. Since m^6A modification is dynamically regulated in vivo, does Mettl3 cooperate with Alkbh5 to regulate the hair cycle and the proliferation phenotype of hair follicle stem cells in mice?

    The reviewer raises an important point that warrants further investigation. The m^6A modification is a dynamically regulated process *in vivo*, and alterations in the balance of m^6A modification play critical roles in maintaining physiological homeostasis and regulating pathological changes. To further explore the role of m^6A modification in HFSCs, we examined the phenotype of *Mettl3* conditional knockout mice. Following tamoxifen induction during the second telogen phase, *Mettl3* was efficiently deleted in HFSCs (Fig 6A). The second hair cycle proceeded normally in these mice; however, we observed that the dorsal hair coat of M3;K5-cKO mice became sparse approximately one month later (Fig 6B).

    We next isolated HFSCs from M3;K5-cKO mice and subjected them to 3D culture. During culture, 4-hydroxytamoxifen was added to the medium to induce *Mettl3* deletion *in vitro*, with DMSO used as the control. RT-qPCR first confirmed efficient induction of *Mettl3* deletion *in vitro* (Fig 6C,D). During culture, we found that *Mettl3* deletion significantly reduced both the colony-forming efficiency and spheroid diameter of HFSCs (Fig 6E,F). Consistently, EdU incorporation assays showed that loss of *Mettl3* decreased the proportion of EdU-positive cells (Fig 6G). Immunofluorescence staining for SOX9 and CD34 indicated that *Mettl3* deletion did not affect the maintenance of HFSC stemness under *in vitro* culture conditions (Fig S6A). These results suggest that METTL3 promotes HFSC proliferation. To determine whether METTL3 regulates HFSC growth through an m^6A-dependent mechanism, we used STM2457, a small-molecule inhibitor reported to specifically inhibit the methyltransferase activity of METTL3. Compared with control cells,

STM2457-treated HFSCs exhibited markedly impaired growth (Fig 6H,I). Therefore, we believe that METTL3 regulates HFSC growth through an m^{6}A-dependent mechanism. These new data have been added to the revised manuscript as Figure 6 and Figure S6.

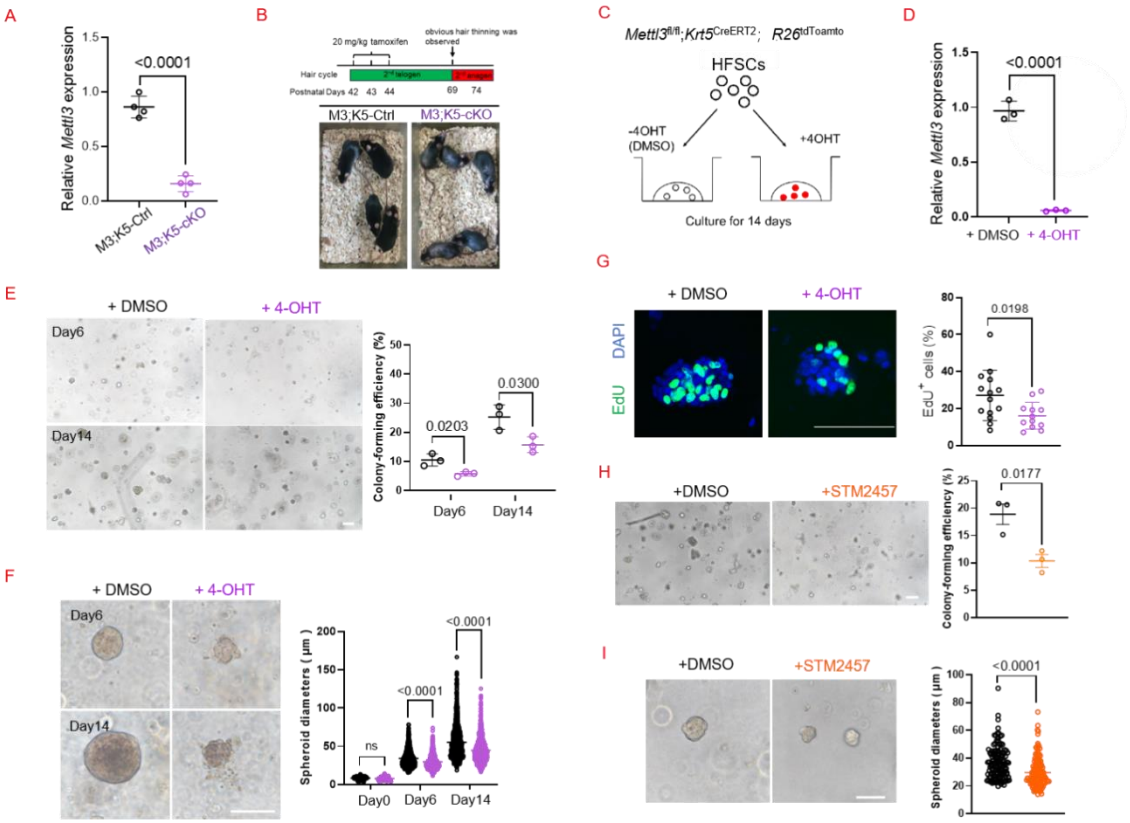

Figure 6 *Mettl3* deletion inhibits hair growth and HFSC proliferation in mice

Figure 6 *Mettl3* deletion inhibits hair growth in vivo and HFSC proliferation by m^{6}A modification-dependent in vitro. (A) RT-qPCR analysis of *Mettl3* expression in HFSCs isolated from M3;K5-Ctrl and M3;K5-cKO mice one week after tamoxifen nasal instillation. (B) *Mettl3*$^{fl/fl}$; *Krt5*^{CreERT2} and *Krt5*^{CreERT2} mice were treated with tamoxifen by nasal instillation for three consecutive days at the second telogen of the hair follicle cycle in mice (P42). Hair thinning was observed one month after tamoxifen administration. (C) Schematic diagram of the experimental workflow. HFSCs were sorted from *Mettl3*$^{fl/fl}$; *Krt5*^{CreERT2}; *Rosa26*^{tdTomato} mice without prior tamoxifen-induced recombination and embedded in Matrigel for *in vitro* 3D culture. Cells were cultured in medium without 4-OHT as the control group or in medium containing 4-OHT to induce Mettl3 deletion. (D) RT-qPCR analysis of Mettl3 expression in *in vitro*-cultured control and Mettl3-knockout HFSCs. (E) (Left) Bright-field images of control and *Mettl3*-knockout HFSCs on days 6 and 14 of *in vitro* culture. Right, quantification of the percentage of colony-formation efficiency on days 6 and 14. Scale bar, 100 μm. (F) (Left) Bright-field images of control and Mettl3-knockout HFSCs on days 6 and 14 of *in vitro* culture. Right, quantification of HFSC spheroid diameters on day 0, 6 and 14. Scale bar, 50 μm. (G) (Left) EdU fluorescence staining showing proliferation of *in vitro*-cultured control and Mettl3-knockout HFSCs. Right, quantification of the percentage of EdU-positive cells in each HFSC spheroid. Scale bar, 50 μm. (H) (Left) Bright-field images of control and STM2457-treated HFSCs on day 14 of in vitro

culture. Right, quantification of the percentage of colony-formation efficiency on day 14. Scale bar, 100 μm. (I) (Left) Bright-field images of control and STM2457-treated HFSCs on day 14 of *in vitro* culture. Right, quantification of HFSC spheroid diameters on day 10. Scale bar, 50 μm. Bars represent mean ± SD.

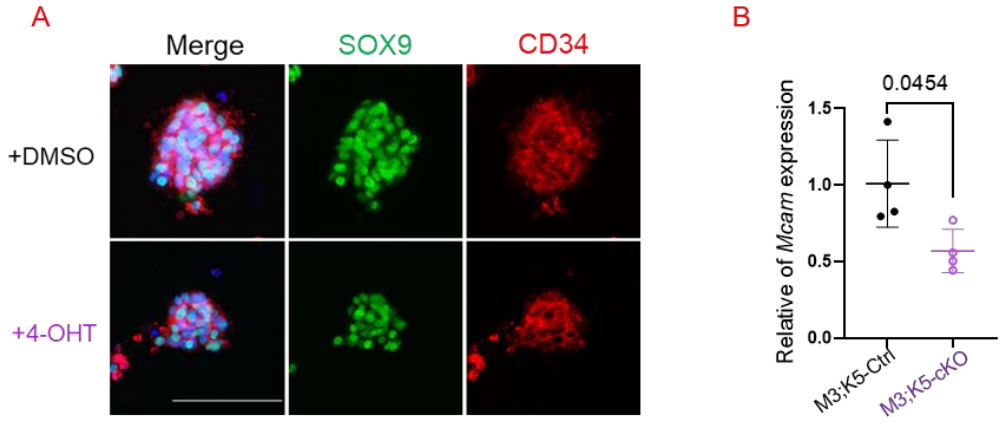

Figure S6 *Mettl3* deletion does not affect the maintenance of HFSC, and downregulates Mcam expression. (A) Immunofluorescence staining for DAPI (blue), SOX9 (green), and CD34 (red) to evaluate the stemness of *in vitro*-cultured HFSCs. Scale bar: 50 μm. (B) RT–qPCR analysis of *Mcam* mRNA expression in HFSCs from M3;K5-Ctrl and M3;K5-cKO (n = 4) mice. Bars represent mean ± SD.

2. Is Mcam a target gene jointly regulated by Mettl3 and Alkbh5?

   We thank the reviewer for this helpful comment. We sorted HFSCs from M3;K5-Ctrl and M3;K5-cKO mice and examined *Mcam* expression by RT-qPCR. The results showed that Mettl3 deletion increased *Mcam* expression (Fig S6B). Therefore, Alkbh5 and Mettl3 may jointly regulate *Mcam* expression.

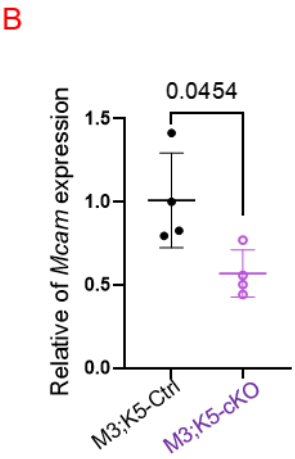

Figure S6 *Mettl3* deletion does not affect the maintenance of HFSC, and downregulates *Mcam* expression. (B) RT–qPCR analysis of *Mcam* mRNA expression in HFSCs from M3;K5-Ctrl and M3;K5-cKO (n = 4) mice. Bars represent mean ± SD.

3. Does Alkbh5 knockout promote periodic activation and proliferation of hair follicle

stem cells in mice, and could this ultimately result in an exhausted hair follicle stem cell pool?

The reviewer raises an important question, as stem cell exhaustion is a critical topic in the field of stem cell regeneration. First, the enhanced activation and proliferation of HFSCs caused by *Alkbh5* deletion are consistent with changes in the hair cycle and do not represent continuous proliferation. Second, we performed long-term monitoring of hair cycle progression in the same mice. The results showed that, regardless of *Alkbh5* deletion, HFSCs still underwent cyclic activation and proliferation (Fig. S1C). Based on these findings, we believe that *Alkbh5* deletion does not lead to exhaustion of the HFSC pool.

4. Please perform experiments by testing if MCAM knockdown suppresses Wnt target genes (e.g., Axin2, Cyclin D1) or alters β-catenin localization in HFSCs.

   We thank the reviewer for this helpful comment. Through Mcam knockdown experiments, we found by RT-qPCR that, after WNT1 treatment, the expression of Wnt signaling target genes, including *Ccnd1*, *Ccnd2*, and *Ppard*, was suppressed, as shown in Fig 5H.

H

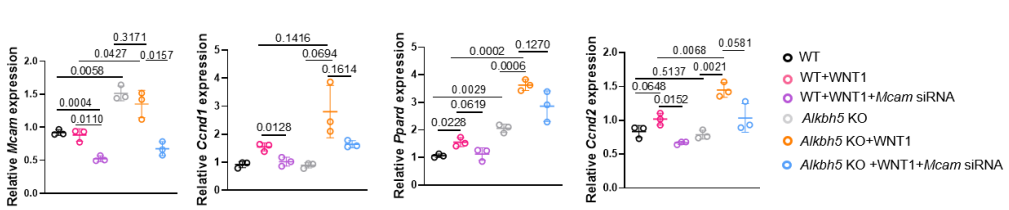

Figure 5 MCAM promotes hair follicle stem cell proliferation. (H) RT-qPCR analysis of the expression levels of the Wnt target genes *Ccnd1*, *Ccnd2*, and *Ppard* in A5;K5-Ctrl, A5;K5-cKO, *Mcam*-knockdown A5;K5-Ctrl, and *Mcam*-knockdown A5;K5-cKO HFSCs under both untreated and WNT1-treated conditions.

5. Please assess MCAM's role in HFSC migration/niche engagement via live imaging or transwell assays.

   We thank the reviewer for this helpful comment. We used a Transwell assay (8.0 μ; Sigma, CLS3422) to examine changes in HFSC migratory capacity after *Mcam* knockdown. HFSCs were isolated by flow cytometry and co-cultured with mitomycin C-treated Swiss 3T3 feeder cells until the cell density reached approximately 50–60%. The cells were then transfected with *Mcam* siRNA using INTERFERin transfection reagent (Polyplus, 101000028) for 48 h. After transfection, cells were dissociated, and 1 × 10^4 cells were seeded into the upper chamber of Transwell inserts in serum-free medium. The lower chamber was filled with culture medium containing 100 ng/mL WNT1 (Gibco, 120-17-10UG). After 48 h of incubation, the migratory efficiency of HFSCs was assessed. We found that *Mcam* knockdown did not result in a noticeable difference in HFSC migration in the

Transwell assay, as shown in Fig R1.

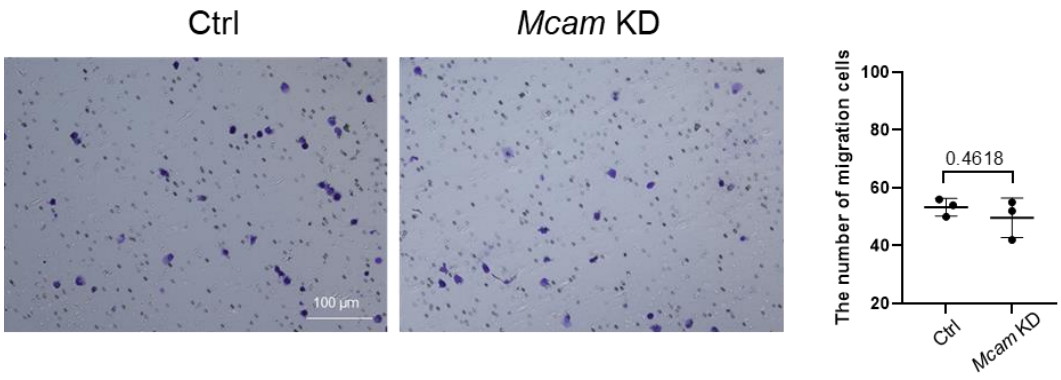

Fig R1: Effect of MCAM knockdown on primary HFSC migration. Representative images (left) and quantification (right) of migrated primary HFSCs. FACS-isolated HFSCs were transfected with control siRNA (Ctrl) or *Mcam* siRNA (*Mcam* KD) for 48 h, and $1x10^4$ cells were seeded into the upper chambers of Transwell inserts. Recombinant WNT1 (100 ng/mL) was added to the lower chambers. After 48 h of incubation, the migratory efficiency was evaluated. Data are presented as mean ± SD from three independent biological replicates (n=3). Scale bar, 100μm.

6. Both Alkbh5 and Fto are demethylases. While the expression of Alkbh5 is shown to change during the transition of the hair follicle cycle in mice, does Fto expression also change during this process?

   We thank the reviewer for this helpful comment. We examined the expression levels of Fto in HFSCs sorted from early and late telogen by RT-qPCR and found no obvious difference in Fto expression between these two time points, as performed in Fig 1A.

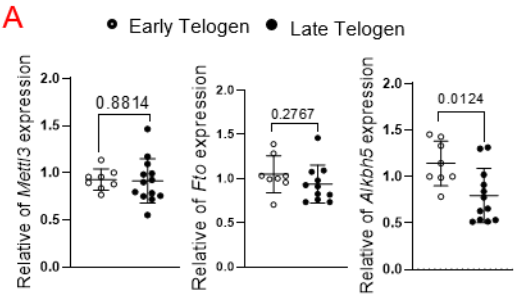

Figure 1 *Alkbh5* knockout promotes telogen-to-anagen transition in hair follicles. (A) RT–qPCR analysis of *Mettl3*, *Fto* and *Alkbh5* transcript levels in mouse epidermal cells at the early (P46, n = 8) and late (P69, n = 13) telogen phases.

7. To validate the consistency of cellular phenotypes in vivo and in vitro, does Alkbh5 knockout affect the apoptosis of hair follicle stem cells in 3D cultures?

We thank the reviewer for this helpful comment. We examined this by performing immunofluorescence staining for cleaved-caspase-3 in HFSCs cultured under *in vitro* 3D conditions. We found that the number of cleaved caspase-3-positive cells was not significantly different between the groups. The results are shown in Fig R2.

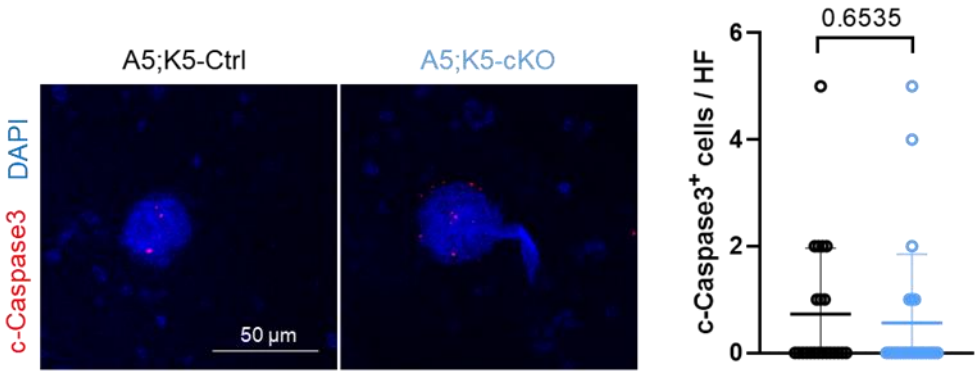

Figure R2. Cleaved-caspase-3 expression in 3D-cultured HFSCs. Representative images (left) and quantification (right) of immunofluorescence analysis of cleaved-caspase3-positive cells in primary HFSCs under in vitro 3D culture conditions. Bars represent mean ± SD (n=3). Scale bar, 50μm.

8. Please specify the number of alopecia areata patient samples used in scRNA-seq analysis to bolster translational claims.

We thank the reviewer for this comment. The alopecia areata patient data used in our study were derived from the clinical single-cell omics dataset reported by Ober-Reynolds B. et al.: "***Integrated single-cell chromatin and transcriptomic analyses of human scalp identify gene-regulatory programs and critical cell types for hair and skin diseases***," Nature Genetics 2023 Aug;55(8):1288–1300. doi: 10.1038/s41588-023-01445-4. This dataset includes samples from 10 healthy individuals and 5 patients with alopecia areata. We have added the corresponding information to the relevant sections of the main text.

1 Andl, T., Reddy, S. T., Gaddapara, T. & Millar, S. E. WNT signals are required for the initiation of hair follicle development. *Dev Cell* **2**, 643-653, doi:10.1016/s1534-5807(02)00167-3 (2002).

2 Kandyba, E. *et al.* Competitive balance of intrabulge BMP/Wnt signaling reveals a robust gene network ruling stem cell homeostasis and cyclic activation. *Proc Natl Acad Sci U S A* **110**, 1351-1356,

doi:10.1073/pnas.1121312110 (2013).
3 Cui, L. *et al.* N6-methyladenosine modification–tuned lipid metabolism controls skin immune homeostasis via regulating neutrophil chemotaxis. *Science Advances* **10**, eadp5332, doi:10.1126/sciadv.adp5332.
4 Hamashima, K. *et al.* Single-nucleus multiomic mapping of m6A methylomes and transcriptomes in native populations of cells with sn-m6A-CT. *Molecular Cell* **83**, 3205-3216.e3205, doi:10.1016/j.molcel.2023.08.010 (2023).
5 Li, Y. *et al.* Systematic evaluation of tools used for single-cell m6A identification. *Communications Biology* **8**, 1841, doi:10.1038/s42003-025-09246-7 (2025).
6 Li, Y. *et al.* Single-cell m6A mapping in vivo using picoMeRIP–seq. *Nature Biotechnology* **42**, 591-596, doi:10.1038/s41587-023-01831-7 (2024).

Author's Response to Review #1：

1. The manuscript must not state "cell-intrinsic" role for ALKBH5 in HFSCs, as the experimental data clearly shows that a broader epidermal deletion using the K5-CreERT2 model results in a much robust phenotype comparing to the HFSC-specific deletion using the Lgr5-CreERT2 model. It is possible that a better experimental design for the deletion of ALKBH5 in HFSCs could result in a similar phenotype to the K5-CreERT2 model, but this was not demonstrated and remains speculative. Since authors used the K5-CreERT2 model throughout majority of their paper, they should adhere to the experimental data in a conservative manner, and this should be reflected in the revised text and discussion more clearly.

   We thank the reviewer for this important comment and agree that our original wording overstated the evidence supporting a strictly "cell-intrinsic" role of ALKBH5 in HFSCs.

   As the reviewer pointed out, deletion of *Alkbh5* using the *Krt5*^{CreERT2} model resulted in a more pronounced phenotype than deletion using the HFSC-specific *Lgr5*^{CreERT2} model. We agree that these findings indicate that additional epidermal cell populations targeted by *Krt5*^{CreERT2} may contribute to the observed phenotype, and therefore our data do not definitively establish that the effects of ALKBH5 are exclusively HFSC-autonomous.

   To address this concern, we have carefully revised the manuscript and toned down statements referring to ALKBH5 as a "cell-intrinsic", "intrinsic licensing", or "intrinsic checkpoint" regulator. Throughout the revised manuscript, these terms have been replaced with more conservative descriptions such as "regulatory factor", "factor regulated cell state changes", or "factor involved in the telogen-to-anagen transition", which more accurately reflect the scope of our experimental evidence.

   We appreciate the reviewer's suggestion and believe that these revisions provide a more balanced interpretation of our findings and better align our conclusions with the experimental data.